SURFACE SKIMMING BULK WAVES, SSBW

Meirion Lewis, Royal Signals and Radar Establishment, Malvern, Worcs, U.K.

ABSTRACT In this paper we review the properties of a relatively new class of planar acoustic wave component employing surface skimming bulk waves, SSBW. In SSBW devices the input interdigital transducer launches a horizontally-polarised bulk wave which is beamed along the surface, and is received by the output transducer long before it reaches any other surface of the substrate. Devices employing SSBW therefore superficially resemble SAW devices, and retain many of their attractions, eg planar construction and design flexibility. In addition, however, SSBW possess a number of practical advantages over SAW, especially for use in narrow band filters and oscillators. These include:- (i) higher velocity and lower propagation losses which enable operation up to about 1.6 times the highest SAW frequency on ST-quartz, (ii) superior temperature coefficients, and (iii) insensitivity to surface contamination. The first part of this paper reviews the basic properties of SSBW, including theoretical and experimental aspects of SSBW propagation, and the attractive properties of SSBW devices. The second part reviews the use of antenna theory to explain the insertion loss and frequency response of SSBW devices, and the electrical characteristics of SSBW transducers.

Introduction

The interdigital transducer, IDT, was first introduced by Mortley[1] for the transduction and reception of bulk acoustic waves travelling through the volume of a 3-dimensional solid sample. In such devices the acoustic wave is launched at an angle θ to the surface when the phase-matching condition of Eq (1) is satisfied

$$p \cos\theta = \lambda \qquad \text{.....(1)}$$

where p is the period of the IDT and λ the acoustic wavelength:

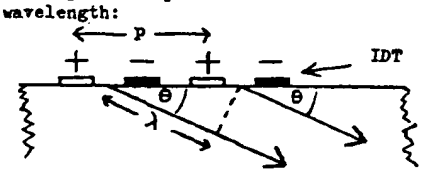

FIGURE 1

It was subsequently discovered by White and Voltmer[2] that the IDT is also an efficient generator of surface acoustic waves, SAW, and this led to the development of a novel generation of planar acoustic wave devices, the properties of which are well covered in the proceedings of this conference from c. 1972 to date. From the foregoing it is hardly surprising that one problem encountered in SAW devices arises from the generation by the IDT of unwanted bulk waves. These waves interfere with the SAW response by travelling directly to the output IDT (θ~0 in Fig. 1) or by reflection from other surfaces of the substrate. A recent review of the situation has been given by Milsom[3]. There are in the literature numerous other references to such unwanted bulk waves, and our refs (4) to (8) are but a few of the more important papers. Most of these papers are concerned with the deleterious effects of such bulk waves in SAW devices, especially broadband filters. In contrast, as we shall see, surface-skimming bulk wave (SSBW) devices employ such bulk waves rather than SAW to perform the required signal processing function. In the first part of this paper we review the basic properties of SSBW, and describe certain orientations of quartz and $LiTaO_3$ with very attractive properties from the viewpoint of SSBW devices. In the second part of the paper we review the use of antenna theory to explain the detailed electrical peroperties of SSBW transducers and filters.

Part 1: Basic Properties of SSBW

First observations of SSBW

Our work has been principally in the field of SAW oscillators, in which the SAW element is a narrow-band filter with prescribed phase and amplitude response. In such narrow-band components the effect of the bulk wave excitation is to introduce separate passband(s) of similar shape to the SAW passband, but at higher frequencies [6,9], see Fig. 2(a). As discussed later these passbands are caused by those bulk wave(s) that can propagate with k-vector parallel to the surface while satisfying the surface boundary conditions. Such surface skimming bulk waves, SSBW, travel with velocity (c) and attenuation essentially unchanged from their values in the infinite medium, and the passband frequencies, f, are given by $f = c/p$, corresponding to $\theta = 0$ in Eq (1). In all cases studied to date this relationship has been found to hold. Further experimental confirmation of the bulk wave nature of the responses is obtained by adding absorber to the surface between the IDT's; the SAW response is heavily attenuated, but the SSBW responses little affected, Fig 2 (b). In ref (9) it is further shown conclusively (by roughening and rotating the lower face of the substrate) that the SSBW travel directly from the input to output IDT, Fig 3, rather than by reflection from the lower surface of the substrate.

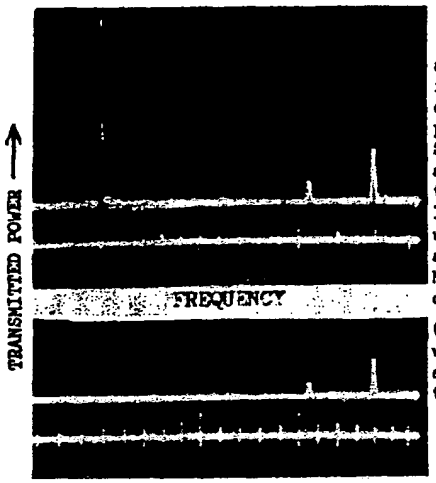

FIGURE 2
(a) Response of a SAW oscillator filter on AT-quartz with x-propagation. The SAW response is at 170MHz, the fast transverse and longitudinal bulk wave responses are at 275 and 309 MHz. Markers occur every 10MHz.
(b) as (a) but with absorber added between the IDT's.

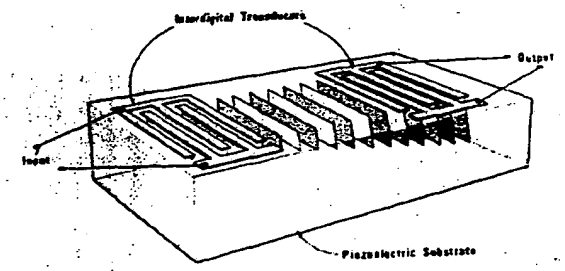

FIGURE 3. Schematic view of SSBW device.

In part 2 we show that the operation of SSBW is readily explained in terms of antenna theory, the IDT's acting as endfire array antennas. Meanwhile, however, we must consider how the SSBW energy is able to radiate between such antennas, unperturbed by the presence of the free surface of the substrate.

1977 Ultrasonics Symposium Proceedings
IEEE Cat # 77CH1264-1SU

Theoretical aspects of SSBW propagation

It is by no means obvious that a wave can emanate from the I.D.T. in the form shown in Fig. 3, for such a radiation pattern has a strong $\underline{k}$-component parallel to the surface ($\theta = 0$) and obviously involves a mechanical disturbance at the surface. In general such a disturbance is not compatible with the stress-free boundary conditions obtaining at the surface. In order to discover suitable orientations for SSBW propagation we have therefore adopted a search procedure[10] which is closely analogous to the SAW search procedure[11]. In this approach we choose a substrate orientation and assume a form for the mechanical disturbance. We then examine the three stress components at the surface, and only if all three vanish simultaneously do we conclude that we have found a suitable orientation for SSBW propagation. In the present case we assume that a wave can propagate with $\underline{k}$ parallel to the surface and with identical displacement components to one of the three bulk waves which can propagate with the same $\underline{k}$-vector in the infinite medium. To date the only waves we have identified which do satisfy the boundary conditions are certain shear waves polarised parallel to the surface of the substrate (ref 10, appendix I). This finding is consistent with the work of Mitchell[7]. We have therefore confined our investigations to substrate orientations supporting such horizontally-polarised shear waves.

We need hardly add that there exist other waves which can travel a finite distance, say 100λ, with little attenuation even though they do not exactly satisfy the boundary conditions; an example is the longitudinal wave on the x-axis of AT-quartz, Fig. 2. The possibility of using such waves in devices deserves further consideration.

On the experimental side we have verified the free propagation of SSBW as sketched in Fig. 3 by impulsing a 3-finger-pair IDT (with aperture 200λ) and monitoring the acoustic intensity at the surface by means of similar IDT's placed every 20λ along the path. The monitored signal varied as [10]

$$\left.\begin{array}{ll} \text{power} & P = P_o\,(\lambda/R) \\ \text{voltage} & V = V_o\,(\lambda/R)^{\frac{1}{2}} \end{array}\right\} \qquad \ldots\ldots\ldots\ldots (2)$$

where R is the pathlength travelled. The variation in Eq (2) is that expected for radiation from a line source, assuming that the propagation is unperturbed by the surface. In this experiment the substrate orientation was one chosen for its SSBW properties, namely AT-quartz with $\underline{k}$ perpendicular to the x-axis. As discussed in part 2, and in ref (12), further confirmation of the free propagation of SSBW comes from the excellent agreement between device responses and IDT radiation resistances that are (a) measured, and (b) calculated assuming Eq (2).

The attractions of SSBW devices

The principal attractions of SSBW devices are very similar to those of SAW devices, viz they provide small, cheap, rugged, planar components with great design flexibility. In addition, however, SSBW offer a number of advantages over SAW for certain applications:-

(i) Bulk waves have higher velocities and can therefore be used to higher frequencies than SAW. This is evident from Fig. 2, and has allowed us to produce devices at frequencies up to 2.3 GHz[10].

(ii) Bulk waves suffer lower propagation losses than SAW, an important consideration at microwave frequencies.

(iii) Bulk waves have superior temperature coefficients to SAW in both quartz and $LiTaO_3$, which is particularly important in oscillators, resonators, and narrow-band filters. In particular, as shown below, SSBW devices are able to employ the same bulk waves that are excited in conventional AT and BT-cut quartz crystal resonators.

(iv) As is evident from Fig. 2, SSBW are less sensitive to surface contamination than SAW, which should ease the long term ageing problem in oscillators, and generally ease fabrication and packaging problems.

Substrate orientations for SSBW

In seeking suitable orientations to support SSBW we naturally started by considering the most widely used SAW piezoelectric crystals, quartz, $LiNbO_3$ and $LiTaO_3$, and concentrated on substrate orientations supporting a horizontally-polarised shear wave. In addition, we wanted the chosen orientations to satisfy as many as possible of the following criteria.

(a) Large piezoelectric coupling to the horizontally polarized shear wave (SSBW).
(b) Zero beam steering both on the surface and into the volume (SSBW).
(c) Zero temperature coefficient of delay (SSBW).
(d) Zero piezoelectric coupling to SAW.
(e) Zero piezoelectric coupling to other bulk waves, or negligible propagation of these waves for the reasons discussed earlier.

A family of cuts of quartz satisfying most of these criteria is the rotated y-cuts with propagation perpendicular to the x-axis[9]. Here, the SAW coupling vanishes identically, all such cuts support an x-polarised shear wave which suffers no beam steering on the surface, and, for two small ranges of angle of the rotated y-cut, the temperature coefficient of delay is small. These ranges are + 30° to + 40° and -48° to -55° rotated y-cuts. These latter cuts are closely related to the well known AT and BT-cuts of conventional bulk-wave-oscillator crystal, but their roles are inverted because, in SSBW devices, the propagation ($\underline{k}$-vector) is along the surface, rather than perpendicular to the surface. This is illustrated in Fig. 4.

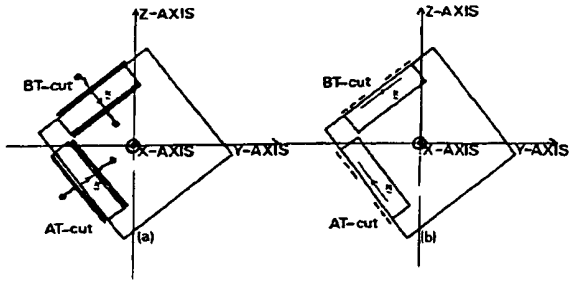

FIGURE 4. Schematic comparison of the use of rotated Y-cut quartz crystals (with propagation perpendicular to the x-axis) in (a) conventional resonators, and (b) SSBW delay lines and resonators. (The AT and BT cuts are not exactly at right angles).

By good fortune, it also happens that these cuts suffer a negligible beam steering into the volume of the material[13], and that the longitudinal wave response is not detectable, so that very 'clean' responses are obtained. Most of our recent studies have therefore concentrated on these two cuts of quartz, especially the AT cut (+35.3° rotated y-cut) which has essentially

zero temperature coefficient of delay at room temperature in our devices, as discussed below.

We have measured the temperature coefficients of frequency (or delay) of the two families of rotated y-cuts (all with $\underline{k}$ perpendicular to the x-axis) covering the ranges +33° to +38°, and -48° to -51½° rotated y-cuts, as these have small temperature coefficients in the range of interest, Fig. 5. The corresponding velocity data is presented in Fig. 6.

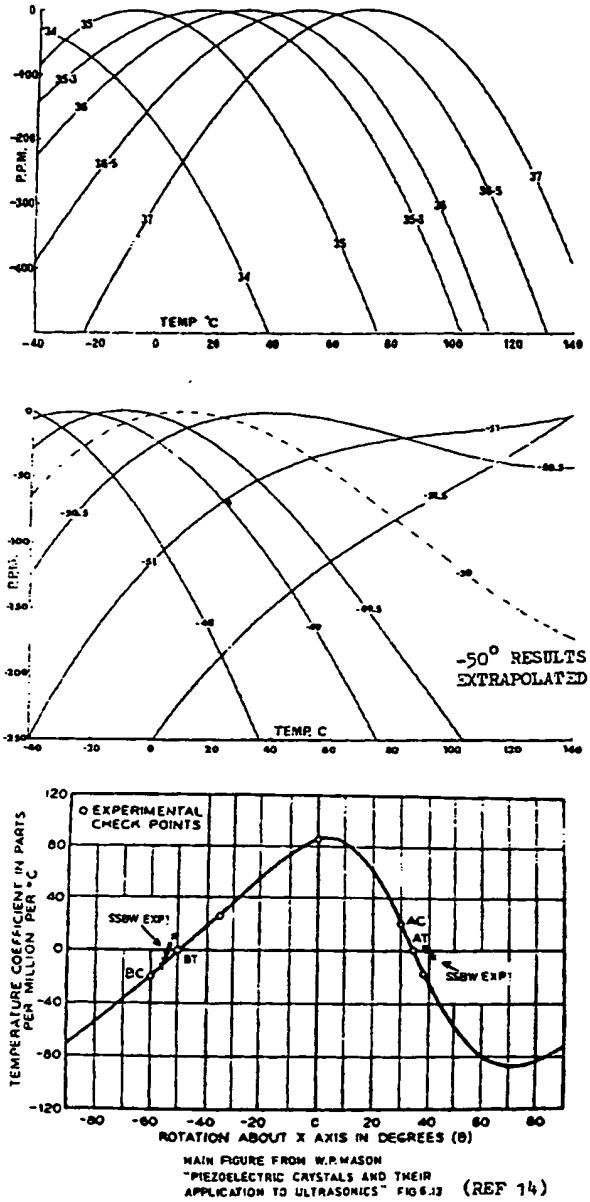

FIGURE 5. (a) and (b): temperature coefficients of frequency of SSBW on various rotated y-cuts of quartz with propagation perpendicular to the x-axis. (c) compares the first-order temperature coefficients of SSBW with conventional resonators, allowance having been made for the 90° difference in $\underline{k}$-vectors (Fig.4).

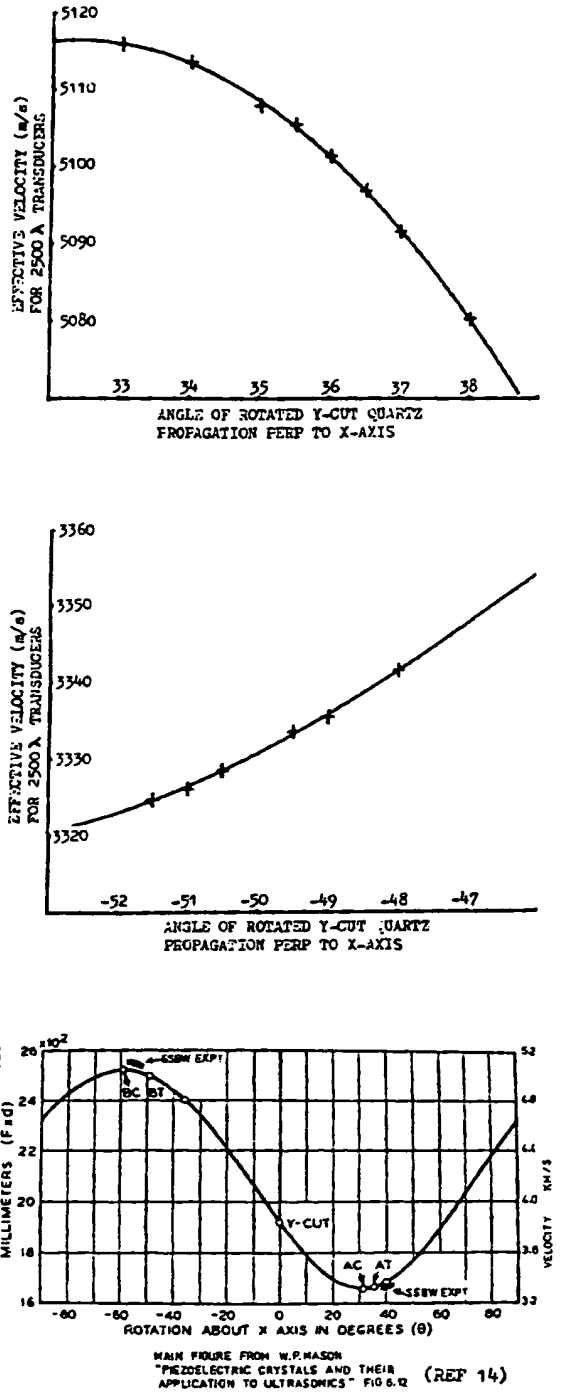

FIGURE 6. (a) and (b): detailed velocity measurements of SSBW on various rotated y-cuts of quartz with propagation perpendicular to the x-axis. (c) compares this velocity data with conventional resonators, allowance having been made for the 90° difference in $\underline{k}$-vectors (Fig. 4).

Figs. 5 and 6 confirm the close relationship indicated in Fig. 4 between the properties of SSBW devices and conventional quartz crystal resonators[14]. In particular, notice that SSBW devices made on substrates close to the -50° rotated y-cut have a cubic frequency-temperature characteristic similar to the well-known AT-cut of conventional quartz crystal. These SSBW characteristics are superior to SAW on ST-quartz. The other cuts of quartz of great importance in SSBW devices are close to the +35° rotated y-cut. Such devices have properties similar to the BT-class of conventional quartz crystal resonator, having a parabolic frequency-temperature characteristic and a velocity of ~5100 m/s. This velocity is 60% higher than SAW on ST-quartz and has enabled us to extend our upper frequency range from 1.4 GHz with SAW devices to 2.3 GHz with SSBW devices[10].

Some experiments involving SSBW on ST-quartz with $\underline{k}$ perpendicular to the x-axis have recently been reported by Yen et al[15]. Since the ST-cut is the +42° rotated y-cut, it is evident that this cut is one particular example of the family of rotated y-cuts described above. These workers have also reported a temperature coefficient of frequency of about 28 ppm/°C for this cut[16], which is quite consistent with our findings in Fig. 5.

It is important to add that the measurements in Figs. 5 and 6 employed an IDT length of $N\lambda = 2500\lambda$, to ensure the excitation of as narrow an acoustic beam as possible. The angular spread of $\underline{k}$-vectors in Fig. 3 is $\theta \sim (2/N)^2$ radians, i.e. $\theta < 2°$ in our devices. In shorter IDT's the results of Figs 5 and 6 may be modified slightly by the excitation of a wider angular spread of $\underline{k}$-vectors.

When we consider $LiNbO_3$ and $LiTaO_3$ we find that these materials have the same elastic symmetry as quartz but they have very different piezoelectric symmetry. This is unfortunate as the family of rotated y-cuts with $\underline{k}$ perpendicular to the x-axis is no longer ideally suited to SSBW applications. We have therefore searched for other orientations in these materials, which satisfy most of the earlier criteria "by accident", rather than by symmetry as was the case for the rotated y-cuts of quartz. To date we have located two suitable cuts of $LiTaO_3$. These employ the two pure shear bulk waves which propagate on the x-axis of $LiTaO_3$ in the infinite medium. One is the +36° rotated y-cut with velocity ~4120 m/s and $\underline{k}$ parallel to the x-axis. The other is the -54° rotated y-cut with velocity ~3460 m/s and $\underline{k}$ parallel to the x-axis. Neither has a particularly good temperature coefficient, but the former has a very high piezoelectric coupling constant for SSBW, suggesting applications in wide-band filters. In each case the piezoelectric coupling to SAW is negligible[17].

Part 2: Application of antenna theory to SSBW devices.

Introduction.

We have seen in part I that if we consider substrates capable of supporting a horizontally-polarized shear wave (SSBW), the acoustic propagation within the substrate is unperturbed by the surface, and in these circumstances we may regard the IDT as an acoustic antenna operating in a half-space. In fact it will make little difference to the arguments if we imagine that another substrate is bonded to the original one, thereby burying the IDT within the medium, and making the problem directly analogous to an e.m. antenna operating in free space. We shall see that it is possible to use many of the results of antenna theory to explain intimate details of the operation of SSBW devices, including

(i) The minimum insertion loss attainable

(ii) The frequency response of SSBW bandpass filters

(iii) The form of the IDT radiation resistance as a function of frequency.

(iv) The variation of radiation resistance (or piezoelectric coupling constant, k^2) with no. of finger pairs, N.

In most of the following we make the assumption that the substrate is isotropic. At least in the case of our "workhorse" material, AT-quartz with $\underline{k}$ perpendicular to the x-axis, this approximation does not seem to introduce any detectable errors. In any case, if we were to attempt to include the anisotropy of real materials in the discussion, the simplicity of the antenna theory approach would disappear. In these circumstances it would be just as easy to use Milsom's rigorous analysis[3].

Elements of Antenna Theory[18]

The basic element of e.m. antenna theory is the elementary dipole radiator, whose radiation pattern resembles a figure '8'. Such dipoles are frequently employed in arrays to add directivity to the antenna as a whole, one such arrangement being the endfire array antenna. To a good approximation the radiation pattern of the entire antenna is the sum of the contributions of the individual elements if their separation is comparable to or greater than the wavelength (ref 18 Ch 5). Furthermore, as the radiation pattern of the array is invariably much narrower than that of the individual elements, the detailed form of the latter is relatively unimportant.

Considering now the IDT as an acoustic antenna, the sources of radiation arise from the complicated electric field patterns in the piezoelectric substrate. Independent of the detailed form of the excitation, an IDT containing N ($\gtrsim 10$) finger pairs is analogous to a (periodic) e.m. endfire array antenna comprising 2N elements, each separated from its neighbours by $\lambda/2$ and with alternate elements driven in antiphase. When driven at the resonant frequency (i.e. such that $p = \lambda$ in Eq (1)) the far-field radiation pattern comprises strong forward and backward lobes of semiangle $\theta \sim (2/N)^2$, (measured to the first zero), together with weaker subsidiary sidelobes. Radiation in the broadside position ($\theta = 90°$ in Eq (1)) vanishes due to cancellation of the various contributions. For an isotropic medium the calculated radiation pattern at resonance is approximately that shown in Fig. 9 (G).

Calculation of the Insertion Loss of SSBW Devices

First consider two idealised ISOTROPIC antennas separated from each other by a distance R large compared with all dimensions of the antennas (including the apertures). Such antennas are obviously located in each other's far field. Imagine that each antenna has its radiation impedance tuned and matched to a source/load impedance. Then for an input power, P(IN), the power density falling on the output antenna is $P(IN)/4\pi R^2$. It is a basic result of antenna theory[18,19] that the effective cross-sectional area of the receiving antenna is $\lambda^2/4\pi$. Therefore the output power is given by

$$P(OUT) = P(IN) \times \frac{\lambda^2}{(4\pi R)^2} \quad \text{(Isotropic antennas)} \qquad \ldots\ldots\ldots\ldots (3)$$

In the case of an IDT operating on resonance, it behaves like an endfire array antenna with its radiation in the forward direction enhanced by the antenna gain, G, which is simply a measure of the directionality, D, of the antenna, i.e. D is the ratio of the intensity in the forward direction to the average intensity over all directions[18,19]. From Ref (18) ch 5, or by direct

calculation on the phased-array model, it can be shown that G is equal to the number of elements in the array, 2N. By reciprocity we must also take account of the antenna gain of the receiver so that the net output power in Eq (3) should be multiplied by $G_1G_2 = 4N_1N_2$.

The final expression for the minimum insertion loss attainable is

$$\frac{P(OUT)}{P(IN)} = \frac{N_1N_2\lambda^2}{4\pi^2R^2} \qquad \text{.....(4)}$$

Evidently to reduce the insertion loss we should increase N_1 and N_2 and reduce R, the optimum arrangement being two identical IDT's placed in close proximity with centre-to-centre separation $R = N_1\lambda = N_2\lambda$. In these circumstances the insertion loss is simply $P(OUT)/P(IN) = 1/4\pi^2$, i.e. 16dB. Obviously it is not strictly permissable to use Eq (4) for the optimum IDT arrangement, as this arrangement violates the far-field assumptions. Nevertheless the argument strongly suggests that low insertion losses are possible, and in practice we have made devices on quartz and $LiTaO_3$ with "tuned and matched" losses of 13dB. This compares with typically 10dB for a SAW device, the extra 3dB in SSBW devices being of little practical significance.

It will be noted that the optimum transducer arrangement described above is exactly that used in single-mode SAW oscillators[20], so that SSBW devices are particularly attractive for oscillator applications[10].

Calculation of the Frequency Response of SSBW devices.

One of the great attractions of SAW devices is the ease with which a given transfer function $H(\omega)$ may be achieved by introducing appropriate weighting into the IDT(s), see for example the bandpass filter section of ref (21). In practice it is often simpler to work in the time domain because the impulse response, h(t), of a given transducer is a replica of the physical construction of the IDT*, which is itself a direct consequence of the independence of the individual finger pairs of the IDT. Of course the frequency response of an IDT, or of a filter comprising two IDT's*, is simply the Fourier transform of the impulse response h(t).

As discussed earlier we believe that the individual finger pairs of a SSBW transducer behave independently (to a good approximation), so that the impulse responses of a SAW device and a SSBW device employing the same IDT pattern should be closely related, (neglecting 2nd order effects such as diffraction on the plane of the substrate). In fact the only difference between the two devices arises because the wavelets excited by the individual finger pairs of the SAW IDT do not spread into the substrate as they travel, the SAW energy being confined to surface. By contrast the local intensity of the SSBW wavelets varies as in Eq (2). A little thought shows that at any instant t_1, the impulse response derives from a number of wavelets all of which have travelled a distance ct_1, and have decayed in amplitude by $(\lambda/ct_1)^{\frac{1}{2}}$. It is therefore evident that the relationship between the SAW and SSBW impulse responses is, neglecting any difference in velocities,

$$h(t)_{SSBW} \propto \frac{h(t)SAW}{\sqrt{t}} \qquad \text{.....(5)}$$

*Footnote: Care should be excercised in discussing the overall response of a filter comprising 2 weighted IDT's, R.H. Tancrell and M G Holland, Proc. IEEE 59 (1971) 393, Fig. 5

where time is measured from the application of the impulse. This important equation is considered in detail in the following paper at this conference[12]. For the present, it is sufficient to note that the factor $\sqrt{t}$ in the denominator of Eq (5) can be made insignificant by increasing the separation of the input and output IDT's. Even when the IDT's are in close proximity the effect of the slowly-varying $\sqrt{t}$-factor is not great. This is illustrated in Fig. 7, which shows the measured and calculated impulse responses of an oscillator filter pattern comprising two identical 100 finger-pair IDT's with centre-to-centre separation of 110λ. The centre frequency of this device is 96.9 MHz, and the tuned insertion loss 13dB. The measured response of a single transducer (calculated by halving the device loss in dB) is shown in Fig 8(a) on a linear scale for comparison with the transducer radiation resistance plots. On the scale shown the response is indistinguishable from the response of the corresponding SAW device, but a more detailed examination shows that the zeroes are somewhat filled in[12]. Such a device is, however, perfectly satisfactory as it stands for use as the feedback element of an oscillator[12,20]. Figs 8 (b) and (c) show the corresponding responses calculated on the RSRE phase-array model and using Milsom's program[3], respectively. The agreement is clearly excellent. These figures also show the corresponding IDT radiation resistances, as discussed below.

Variation of Radiation Resistance with Frequency

Following the work of the Stanford group on SAW IDT's[22] we represent the SSBW IDT electrically by a series combination of its static capacitance, C_o, and a series radiation resistance, R_a, and reactance, X_a. For a weak piezoelectric like quartz with $N \lesssim 300$, we invariably have $1/\omega C_o \gg R_a, X_a$, and it is convenient to assume that such a transducer is driven by a voltage source V, Fig. 10. In these circumstances the current is $i \sim V\omega C_o$, and the total power dissipated in the radiation resistance is

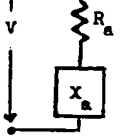

FIGURE 10

$$P = i^2R_a \propto V^2\omega^2C_o^2R_a \qquad \text{.....(6)}$$

It is also clear that the amplitude of each wavelet excited by the IDT is proportional to V, so the total acoustic power radiated is

$$P = V^2I \qquad \text{.....(7)}$$

where I (= $I(\omega)$) is a dimension-less quantity obtained from the phased array model by integrating the bulk wave power radiated over all values of θ(Fig. 1) with unit voltage applied to the IDT. For example, I is very small below the resonant frequency because the phase-matching condition of Eq (1) cannot be satisfied for any value of θ. Comparing the expressions for P in Eqs (6) and (7), it is evident that $R_a(\omega)$ is directly proportional to $I(\omega)$. In Fig. 9 we show on a dB scale the calculated farfield radiation patterns of a 100-finger-pair IDT resonant at 96.9 MHz (cf Figs 7 and 8) when operating at various frequencies from 95.2 to 98.5 MHz. The values of I at each frequency are effectively calculated from the black areas of these radiation patterns, the resulting variation of $R_a(\omega) \propto I(\omega)$ for this phased-array model being plotted in Fig. 8(b).

The result is obviously in close agreement with the measurements, Fig. 8(a), and Milsom's theory, Fig. 8(c). It turns out that the shape of the R_a curve in Fig.8(b) is almost independent of N, and in Fig. 11 we plot a "universal" curve of R_a, with frequencies normalized to

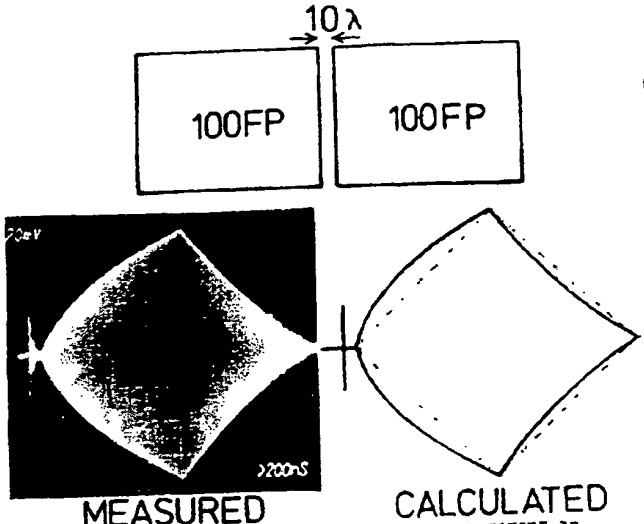

FIGURE 7. top: schematic transducer arrangement in SSBW filter. Substrate AT-quartz with k perpendicular to the x-axis. Centre frequency: 96.9 MHz.

bottom: measured and calculated impulse responses of this device. The dashed curve shows the diamond-shaped impulse response of the corresponding SAW device.

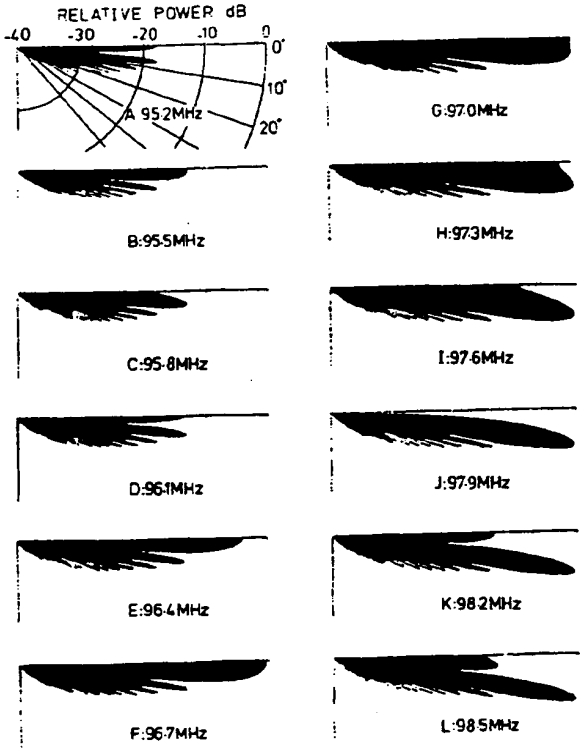

FIGURE 9. Calculated far-field radiation patterns for the input transducer of Fig. 7 at various frequencies from 95.2 to 98.5 MHz. The calculation assumes an isotropic acoustic substrate. Using these plots it is possible to verify the power transmission and R_a curves of Fig. 8(b).

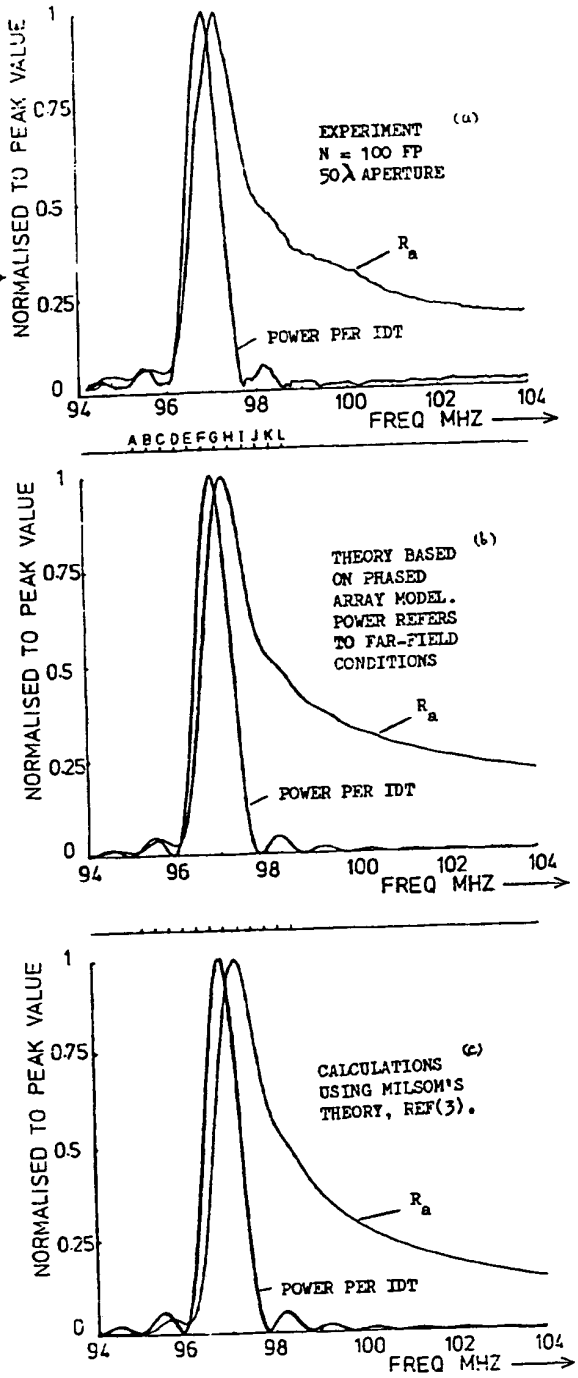

FIGURE 8. Measured and calculated plots of the IDT radiation resistance and power transmission for one IDT of the SSBW filter shown in Fig. 7. The acoustic radiation patterns at frequencies A to L are shown in Fig. 9.

N. Notice that the peak value of R_a (which is ~12% higher than the resonant value) occurs at frequency

$$f_{peak} \sim f_{resonance}\left(1+\frac{0.26}{N}\right) \quad \ldots\ldots\ldots(8)$$

The reason for this is readily seen by comparing Figs 9(G) and (H); in (G) only half a lobe is radiated, while in (H) an almost full lobe is radiated, albeit somewhat narrower.

Variation of Radiation Resistance with N

The previous section may be extended to calculate the variation of R_a with N. Consider first the SAW case. Other things being equal, the amplitude of SAW launched by the IDT is proportional to N, so the power in Eq (7) is $\propto N^2$. Since $C_o \propto N$, it follows on comparing Eqs (6) and (7) that R_a is independent of N[22]. For SSBW, however, the acoustic intensity $\propto N^2$, but the angular width of the main lobe is $\theta \sim (2/N)^{\frac{1}{2}}$, so that $I \propto N^2\theta \propto N^{3/2}$. Comparing Eqs (6) and (7) we find,

$$R_a \propto N^{-\frac{1}{2}} \quad \ldots\ldots\ldots\ldots\ldots(9)$$

In Fig 12 we compare measured values of R_a with calculations based on the above phased-array model, and Milsom's program [3]. The experimental errors are large (due to stray capacitances) but nevertheless confirm the increase in R_a as N is reduced.

At first sight it appears from Fig.12 that the effective k^2 of SSBW on AT-quartz is low, for the 100 finger pair IDT with 50λ aperture has $R_a \sim 9\Omega$; a SAW device on ST-quartz would have $R_a \sim 36\Omega$. However it is not fair to the SSBW device to make such a comparison, because of the higher SSBW velocity (and therefore frequency of operation) and because of the variation of R_a with N in Eq (9). It is more realistic to compare devices in which N has been adjusted to equalize the electrical and acoustic bandwidths[22]. When this is done, we find that SSBW devices on AT-quartz (with k perpendicular to the x-axis) have essentially the same optimised bandwidth as SAW on ST-quartz, i.e. about 5%.

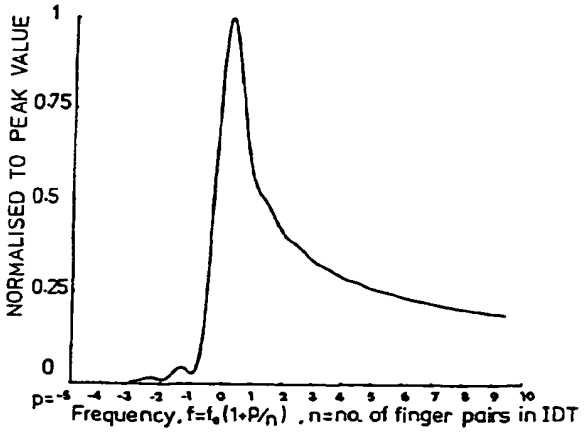

FIGURE 11. 'Universal' radiation resistance curves for a SSBW IDT on an isotropic substrate.

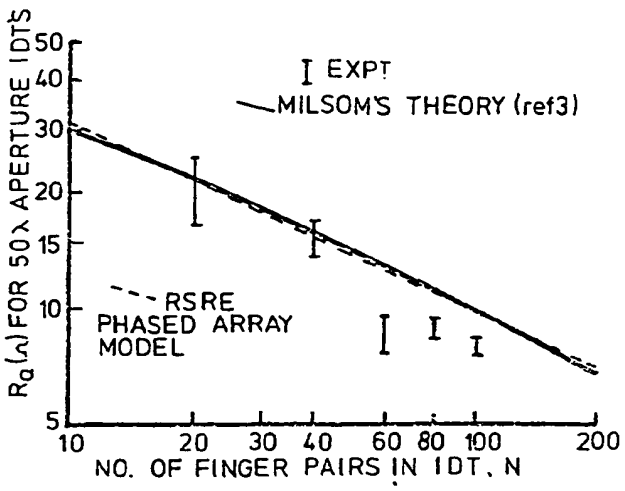

FIGURE 12. Measured variation of R_a with N for IDT's with 50λ aperture on AT-quartz with propagation perpendicular to the x-axis. The theoretical curves employed Milsom's theory (ref 3) and the phased array model.

Conclusions and Discussion

We have described the properties of a new family of acoustic wave device with many of the attractions of surface acoustic wave devices, but with advantages over SAW in certain important aspects. In particular these advantages make SSBW devices of immediate application to bandpass filters as discussed in ref (12), and to high frequency oscillators are discussed in ref (10). For example in Fig. 13 we show the exceptionally smooth passband of a 1.766 GHz SSBW oscillator filter employing a pathlength of 300λ; this was made from a 1.09 GHz SAW oscillator mask.

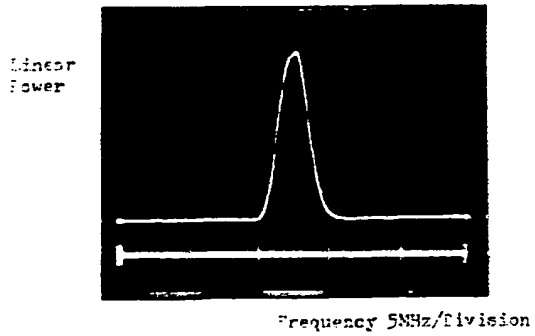

FIGURE 13. Response of a 1.766 GHz SSBW oscillator filter. Untuned loss: 21dB. 10 MHz markers are also visible.

The highest fundamental frequency yet attained is 2.3GHz[10], but we feel that this could readily be extended to >3 GHz by the use of split-finger transducers operating at their 3rd harmonic, see below. In this respect it is important to note that the propagation losses of the SSBW on AT-quartz with k perpendicular to the x-axis are about ⅓rd that of SAW on ST-quartz[23].

One aspect of SSBW that we have not discussed in detail is the absence of spurious responses in our devices. This is apparent from the impulse responses shown in Fig. 7 and from ref (12), but is demonstrated more dramatically in Fig. 14 which shows narrow-band and wideband sweeps of the response of the device illustrated in Fig. 7 when all faces of the substrate (other than that containing the IDT's) are roughened to destroy the coherence of any reflected waves. From this Figure it is clear that the 97 MHz SSBW response is >40 dB above any spurious from 0-500 MHz, apart from low-level 3rd and 5th harmonic responses. Similar results have been obtained with a SSBW device employing split-finger transducers, Fig. 15. More detailed measurements on SSBW transducers employing split-fingers have shown that they behave in a very similar manner to split-finger SAW transducers(6). For example, the effective k^2 is approximately the same for the 1st and 3rd harmonics, and a little less than k^2 at the fundamental of a normal IDT.

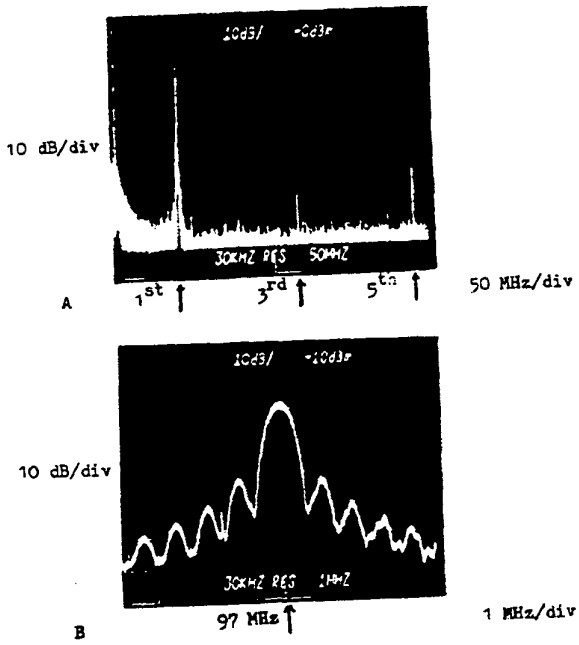

FIGURE 14. (a) broadband sweep (0-500 MHz) of the response of a SSBW filter employing the IDT pattern of Fig. 7.

(b) narrow-band sweep of the main response. (c.f. Fig 8(a)).

Despite the impressive performance of many of the SSBW devices described here, it is apparent that the study of SSBW is still in its infancy, roughly akin in SAW in 1969(22). Judging by the developments in SAW over the past eight years, we may hope to see some spectacular advances in SSBW in the future. Some possible lines of advance are discussed below.

First let us ask how SSBW are related to other acoustic devices. In general terms it is obvious that they attempt to utilise the acoustic modes of propagation of the infinite medium, just as SAW devices attempt to use a mode of propagation on a semi-infinite substrate. In this respect SAW and SSBW differ from many other acoustic devices (resonators, filters) which utilise the normal modes of a finite substrate. Indeed in both SAW and SSBW the presence of other surfaces of the substrate is often an embarrassment, and has to be artificially removed, by rotation, roughening, absorber, etc. (Of course it is relatively easy to absorb/scatter unwanted waves at the higher frequencies contemplated with SSBW, say >1GHz). There are, however, devices in which reflections from other surfaces can be utilized; one example is the resonator of Auld et al(24) and it seems that SSBW are ideally suited to such applications. While on the subject of resonators, we should recall that SSBW resonators employing reflections from an array of surface perturbations have been demonstrated by two groups(10,16). Devices of this kind certainly warrant further investigation.

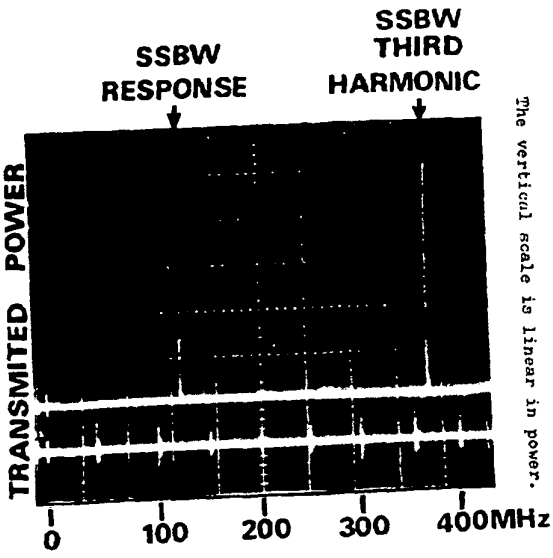

FIGURE 15. Response of a SSBW filter employing split-finger IDT's.

If we examine the particle displacement (polarisation) of SSBW, we realise that SSBW are closely related to Love waves, Bluestein-Gulyaev waves, and waves on corrugated surfaces(24). In all these waves, the acoustic energy is localised at the surface by some slowing mechanism (a slow layer, piezoelectric coupling, or topography, respectively). In SSBW devices we have shown that it is not necessary to use such energy confinement at the surface to produce devices with low insertion losses because the input IDT acts as an endfire array which beams the acoustic energy at the receiving transducer. Nevertheless such SSBW devices are not, as they stand, suitable for use in long delay lines as they suffer an additional 3dB loss for every doubling of the pathlength (Eq.2). In this respect, it may be worthwhile to reconsider the use of some slowing mechanism for SSBW to produce delay lines with, for example, the excellent temperature stability demonstrated in Fig. 5.

This paper has concentrated on the propagation of SSBW on rotated y-cuts of quartz, but other materials/orientation may well have superior properties in some respects. We have already identified two such cuts of $LiTaO_3$(10); these have effective piezoelectric coupling at least as great as SAW on $LiNbO_3$, and are therefore of potential use in wideband filters. Other

materials/orientations might, for example, employ acoustic anisotropy to focus SSBW or beam-steer away unwanted waves, etc. Finally we would like to mention the possibility of applying SSBW to N.D.T., eg for flaw detection on a surface, or just below the surface, for it is clear from the text that unlike SAW, SSBW may penetrate many wavelengths into a substrate. We also hope that another consequence of this penetration is a reduced long-term ageing of SSBW devices, especially oscillators[10].

REFERENCES

1. W Mortley, UK patent 988102 (1962).
2. R M White and F W Voltmer, App. Phys Lett 7 (1965) 314.
3. R F Milsom, Wave Electronics 2 (1976) 64.
4. R V Schmidt, JAP 43 (1972) 2498.
5. M R Daniel and P R Emtage, JAP 43 (1972) 4872.
6. T W Bristol, Proceedings of the International Specialist Seminar on "Component Performance and Systems Applications of SAW devices", Aviemore, UK 1973. IEE Conference publication No 109 pp115-129, especially Fig. 6.
7. R F Mitchell. Proceedings of IEEE Ultrasonics Symposium (IEEE cat 74 CHO 896-1SU) (1974) 313.
8. R S Wagers IEEE Trans SU-23 (1976) 113.
9. T I Browning and M F Lewis, Electronics Letts 13 (1977) 128.
10. T I Browning and M F Lewis, Proceedings of the 31st Annual Frequency Control Symposium, Atlantic City, 1977.
11. T C Lim and G W Farnell, JAP 39 (1968) 4319.
12. T I Browning, D J Gunton, M F Lewis and C O Newton, Next paper in this proceedings.
13. G W Farnell, Can. J Phys 39 (1961) 65, Fig. 2.
14. W P Mason, "Piezoelectric Crystals and their application to ultrasonics" D. Van Nostrand Co (1950) p.99.
15. K H Yen, K L Wang and R S Kagiwada, Electronics Letts 13 (1977) 37.
16. K H Yen et al, proceedings of 31st Annual Frequency Control Symposium, 1977.
17. A J Slobodnick Jr, et al "Microwave Acoustics Handbook, Vol 1A" (1973) p.94.
18. R E Collin and F J Zucker "Antenna Theory, Part I" McGraw-Hill (1969).
19. S A Schelkunoff and H T Friis"Antennas, theory and practice", Wiley, New York, 1952 circa p.44.
20. M F Lewis, Ultrasonics 12 (1974) 115.
21. D P Morgan "SAW passive interdigital devices" IEE reprint series 2 (1976).
22. W R Smith et al. IEEE Trans MTT-17 (1969 865
23. J Lamb and J Richter, Proc Roy Soc A293 (1966) 479.
24. B A Auld et al, Electronics Letts 12 (1976) 650.

Q: Did you try any aging experiments?

A: All I can say is, yes, we did and in the preliminary experiments we did a couple of years ago, they did indeed show an improvement by, I think, 2 to 3 over the surface wave devices that we were aging at the time. Unfortunately, we have not repeated those experiments yet. I can assure you that there are people working hard at it in RSRE but they want to get everything right, the seating of the container, the mounting, etc., and they are just not publishing the results until they're sure that everything else is set up properly. But why I'm pretty sure of that is that it's not going to be any worse in surface waves because of that absense of surface contamination effect in the device.

R. Weglein - Hughes Aircraft - Are metal films affected by the temperature and are there any reflections from the metal on the surface?

A: I honestly can't answer the question with respect to the metal on the surface making the turnover temperature. We have not done measurements, and generally speaking, we don't use transducers that heavily metalize the surface anyway, so I just can't answer that one. But what we do know is that metal on the surface does indeed cause reflections for surface skimming bulk waves not dissimilar from the reflections it causes for surface waves. In other words, if you thicken up the transducers you will find that you get into transducer reflections, etc. Indeed that's how the resonator that we showed works.

A: That's Dick Williamson. Are you ever going to get high Q resonators because most of the energy is going to go past the resonators and get lost. I don't have any affirmative answer to this, but if one goes back to an antenna theory, you can see an array of reflectors providing they have got the right spacing will indeed reflect strongly and so I have hope there that indeed one can get high Q's. Another factor in our favor is the fact that the bulk waves we have have got approximately one third of the material attenuation surface waves, so we've got a factor of 3 in our favor to start with. And another factor which I think is quite important is that if you look at the work that has described, with waves and corrugated surfaces, and after all the reflectors are a corrugated surface, he will show you that in fact your surface skimming bulk wave is effectively turned into a surface wave. It might have a penetration of 10 or 100 wave-lengths or something, but it is in fact confined to the surface. So I think all these factors suggest that we may right well end up with high Q resonators if that's what you're after.